Resting-State Cortico-Thalamic-Striatal Connectivity Predicts Response to Dorsomedial Prefrontal rTMS in Major Depressive Disorder

Tim V Salomons[1,2,3,7], Katharine Dunlop[1,4,7], Sidney H Kennedy[2,5], Alastair Flint[2,5], Joseph Geraci[2,6], Peter Giacobbe[1,2,5] and Jonathan Downar*[1,2,5]

[1]MRI-Guided rTMS Clinic, Toronto Western Hospital, Toronto, ON, Canada; [2]Department of Psychiatry, University Health Network, Toronto, ON, Canada; [3]School of Psychology and Clinical Language Sciences, University of Reading, Reading, UK; [4]Faculty of Arts and Sciences, University of Toronto, Toronto, ON, Canada; [5]Department of Psychiatry, University of Toronto, Toronto, ON, Canada; [6]Department of Pathology and Molecular Medicine, Queen's University, Kingston, ON, Canada

Despite its high toll on society, there has been little recent improvement in treatment efficacy for major depressive disorder (MDD). The identification of biological markers of successful treatment response may allow for more personalized and effective treatment. Here we investigate whether resting-state functional connectivity predicted response to treatment with repetitive transcranial magnetic stimulation (rTMS) to dorsomedial prefrontal cortex (dmPFC). Twenty-five individuals with treatment-refractory MDD underwent a 4-week course of dmPFC-rTMS. Before and after treatment, subjects received resting-state functional MRI scans and assessments of depressive symptoms using the Hamilton Depresssion Rating Scale (HAMD$_{17}$). We found that higher baseline cortico-cortical connectivity (dmPFC-subgenual cingulate and subgenual cingulate to dorsolateral PFC) and lower cortico-thalamic, cortico-striatal, and cortico-limbic connectivity were associated with better treatment outcomes. We also investigated how changes in connectivity over the course of treatment related to improvements in HAMD$_{17}$ scores. We found that successful treatment was associated with increased dmPFC-thalamic connectivity and decreased subgenual cingulate cortex-caudate connectivity, Our findings provide insight into which individuals might respond to rTMS treatment and the mechanisms through which these treatments work.
Neuropsychopharmacology (2014) 39, 488–498; doi:10.1038/npp.2013.222; published online 23 October 2013

Keywords: major depression; prefrontal cortex; rTMS; neurostimulation; biomarkers

INTRODUCTION

Major depressive disorder (MDD) has a devastating effect not only on symptomatic individuals but also on society as a whole, through high medical costs and loss of productivity (Murray and Lopez, 1996; Collins *et al*, 2011). Despite the enormous societal burden, recent history has seen relatively little progress in treatment efficacy, with the most common non-invasive treatments continuing to demonstrate relatively low response and remission rates (Papakostas *et al*, 2007; Imel *et al*, 2008; Gartlehner *et al*, 2011; Spielmans *et al*, 2011). There have been calls for personalized treatment approaches to improve response rates (Collins *et al*, 2011; Kapur *et al*, 2012).

One approach to developing personalized treatment approaches is to better understand the biology that may underlie individual differences in response to treatment. Biomarkers that distinguish between depressed and non-depressed individuals have been identified at the neural level (Drevets *et al*, 2008; Northoff *et al*, 2011) but less is known about the heterogeneity that underlies individual differences in treatment response in depressed individuals. Several studies report an association between activation in single neural regions and treatment response. In particular, responses in pre- and subgenual cingulate and adjacent ventral medial prefrontal cortex (vmPFC) have been associated with response to cognitive behavioral therapy (Ritchey *et al*, 2011; Siegle *et al*, 2006), antidepressant medication (Davidson *et al*, 2003; Kennedy *et al*, 2001, 2007; Mayberg *et al*, 1997; Pizzagalli *et al*, 2001), and repetitive transcranial magnetic stimulation (rTMS) (Li *et al*, 2010). More recent work has focused on resting-state connectivity, based on the presumption that activity across widespread networks will be more telling than that of single regions. Consistent with studies implicating pre- and subgenual cingulate, recent findings suggest that connectivity between ventral and dorsal regions of the anterior cingulate cortex predicts response to antidepressant medication (Kozel *et al*, 2011).

If this functionally connected network represents a window into the neural networks that underlie treatment success, several clinically important questions arise. The first is whether directly stimulating constituent regions of this putative treatment response network might result in improved outcomes. One way to examine this question is through the use of repeated transcranial magnetic stimulation (rTMS), an evolving treatment for refractory depression that uses magnetic fields to stimulate focal cortical regions with electrical current. Although rTMS treatment for depression has primarily focused on the dorsolateral prefrontal cortex (dlPFC), convergent evidence from lesion and structural imaging studies suggests that the dorsal medial prefrontal cortex (dmPFC) might have a more central role in emotion regulation and the pathophysiology of major depression (Downar and Daskalakis, 2012). Given the spatial resolution of rTMS and the proximity of this region to the dorsal cingulate, using this target may have the added advantage of demonstrating how direct stimulation of constituent regions of the outcome-predicting network identified by Kozel et al (2011) might address the pathophysiology of depression, both at the neural and behavioral level.

Here we investigated the neural and behavioral response to rTMS applied to dmPFC. We observed substantial heterogeneity in the degree of treatment response. We then investigated the neural correlates of this heterogeneity using resting-state functional connectivity. Our primary question was whether baseline resting-state connectivity of the dmPFC and subgenual cingulate cortex (sgACC) predicted response to dmPFC-rTMS. Our secondary question was whether changes in the connectivity of these regions were associated with treatment response.

MATERIALS AND METHODS

Design Overview

Participants diagnosed with unipolar (MDD) or bipolar depression (BD), resistant to at least two trials of medication, were treated with 20 sessions (4 weeks/5 sessions/week) of open-label, add-on rTMS of the bilateral dmPFC. rTMS coil placement for dmPFC stimulation was defined for each subject using anatomical magnetic resonance images acquired a week before treatment, as below. The 17-item Hamilton Depression Rating Scale (HAMD$_{17}$) was used as the primary outcome measure in this study and was administered at baseline and after the conclusion of the course of treatment. Pretreatment resting-state functional connectivity maps for seed regions representing the stimulated dmPFC region were analyzed to identify predictors of HAMD$_{17}$ improvement following treatment. To assess neural correlates of the degree of improvement over the course of treatment, we also conducted a second neuroimaging session in the week immediately following the conclusion of the treatment course.

Subjects

Subjects were 25 patients (10 male; mean 42.6 years, range 19–70) with either unipolar or bipolar illness ($n = 4$; one type one, three type two) and a diagnosis of a major depressive episode resistant to $\geqslant 2$ medication trials or medication intolerance. At the time of study, 7 subjects were taking SSRIs, 9 SNRIs, 4 bupropion, 2 trazodone, 1 mirtazapine, 2 monoamine oxidase inhibitors, 1 tricyclic, 10 antipsychotics, 1 anticonvulsants, 7 benzodiazepines, 6 stimulants, and 3 sleeping pills. Three subjects were taking no psychiatric medications; 18 were taking more than one of the above listed medications. All patients had maintained stable doses of antidepressant medications for at least 4 weeks before treatment and until completing the course of rTMS. The group of subjects who underwent neuroimaging was the latter individuals within a larger 47-patient clinical outcomes case series, which will be reported separately. This convenience sample was chosen entirely based on the availability of functional neuroimaging, with no systematic selection based on clinical or demographic characteristics. Baseline symptom severity on HAMD$_{17}$ was 21.3 (± 6.7 SD) with average length of current episode 42.5 months ($+/- 10.26$ SE). The median length of current episode was 12 months (range 1–204 months). No participants with active substance abuse or psychotic disorders participated in the study. Participants with potential contraindications to rTMS and/or neuroimaging were excluded from participating in this study. All patients provided informed consent to treatment, and the study was approved by the UHN REB.

MRI Acquisition and Neuronavigation

In the week before treatment, subjects underwent MRI on a 3T GE Signa HDx scanner equipped with an 8-channel phased-array head coil. The session included a T1-weighted fast spoiled gradient-echo anatomical scan (TE = 12 ms, TI = 300 ms, flip angle = 20°, 116 sagittal slices, thickness = 1.5 mm, no gap, 256 × 256 matrix, FOV = 240 mm). Patients also underwent a 10-min functional MRI scan (TE = 30 ms, TR = 2000 ms, flip angle = 85°, 32 axial slices, thickness = 5 mm, no gap, 64 × 64 matrix, FOV = 220 mm, 300TRs, 2 s temporal resolution) conducted in the resting state with the eyes closed. In the week after treatment, they also underwent a repeat session with identical parameters, except for abbreviation of the T1 series (80 sagittal slices, thickness = 2 mm, no gap, 96 × 96 matrix, FOV = 200 mm). One subject's time 2 data were lost, so analyses of pre- vs post-rTMS neural change are based on an $n = 24$.

Neuronavigation used the Visor 2.0 system (Advanced Neuro Technologies, Enschede, the Netherlands) for MRI preprocessing. Segments were then used for anatomical landmarking, registration into standard Talairach and Tournoux space, and the construction of 3-D surfaces for the scalp and brain. Sterotactic coordinates were used to identify stimulation area and closest approximately scalp point in standard space (brain coordinate = X 0, Y + 30, and Z + 30; scalp coordinate = X 0, Y + 60, and Z + 60) for coil vertex placement. 3-D brain surfaces corresponding to stimulation coordinates were then coregistered to the patient's head for individualized placement of the rTMS stimulation coil.

rTMS Treatment

A full description of the dmPFC-rTMS treatment protocol has been previously published (Downar et al, 2012). In

brief, rTMS treatment was conducted using a MagPro R30 rTMS system (MagVenture, Farum, Denmark), and Cool-DB80 stimulation coil placed over the dmPFC under MRI neuronavigation as above. Bilateral stimulation of the left then the right hemisphere was accomplished by orienting the coil laterally, with vertex current flow directed toward the hemisphere to be stimulated (Harmer et al, 2001; Terao et al, 2001). Stimuli were delivered at 120% of the resting motor threshold (determined using stimulation of the medial aspect of the primary motor cortex to activate the extensor hallucis longus-EHL), at 10 Hz, at a duty cycle of 5 s on, 10 s off for a total of 3000 pulses in 60 trains per hemisphere per session. Note that the standard safety tables for rTMS administration specify a slightly shorter duration limit of 4.2 s for 10 Hz stimulation at 120% resting motor threshold (Chen et al, 1997). Note also that these safety parameters were based on observations during stimulation of the upper extremities rather than the lower extremities as in the present study (see Supplementary Methods for additional methodological and safety information).

Preprocessing

Preprocessing of resting-state functional data was performed using FEAT (Beckmann et al, 2003), part of FSL. The first five volumes were deleted to account for signal stabilization. Slice-timing correction, removal of non-brain using BET (Smith, 2002), motion correction with MCFLIRT (Jenkinson et al, 2002), and spatial smoothing using a Gaussian kernel of 6 mm FWHM were conducted. Mean-based intensity normalization of all volumes was conducted. Motion parameters and FAST (Zhang et al, 2001) segmented CSF, and white matter mean time series data were extracted and utilized in a linear regression analysis (Fox et al, 2005). Data were bandpass filtered between 0.009 and 0.09 Hz and registered to the MNI-152 template brain using a linear transformation in FSL's FLIRT module.

Seed ROI Selection

Two seed regions of interest (ROIs) in the dmPFC were initially selected based on their proximity to the region stimulated by rTMS. The more superior of the two was just above the cingulate cortex; the second region was deeper, in the region of the anterior midcingulate (aMCC) (Supplementary Figure S2). Time courses for these ROI seeds were extracted from regions defined from a parcellation map established by Craddock et al (Craddock et al, 2012) (see Supplementary Methods for details).

The subgenual cingulate has been consistently linked with outcome prediction (Davidson et al, 2003; Kennedy et al, 2001; Kozel et al, 2011; Mayberg et al, 1997; Ritchey et al, 2011; Siegle et al, 2006) and connectivity with our anatomically defined ROIs was found to predict outcomes in the present study (see Results). We therefore also tested a functionally defined sgACC seed ROI to examine how connectivity of this region was associated with outcomes following rTMS of dmPFC. Thus, although the particular cluster was chosen *post hoc*, there was a strong *a priori* interest in examining this region's role in predicting treatment response.

Statistical Analysis

Seed ROIs were registered to each participant's brain using the transformation matrix from the original registration to standard space in FLIRT, extracting a mean time series of the masked seed ROI region, and analyzed in multiple linear regression analyses to find positively and negatively correlated voxels associated with the seed ROI. This correlation with the time series was taken as a measure of functional connectivity with the seed region. In order to find regions where correlation with the time series of our ROI regions was associated with symptom change following treatment, group level analysis was conducted using the FSL's FLAME mixed effects model (Beckmann et al, 2003), using demeaned $HAMD_{17}$ change scores for each subject as a regressor in the general linear model. All corrections for multiple comparisons were performed using a Gaussian random field theory cluster-based correction ($Z > 1.98$, cluster significance $P < 0.05$, corrected), resulting in corrected z-score maps correlating pretreatment functional connectivity for each seed to $HAMD_{17}$ change.

In order to examine the association between change in functional connectivity and $HAMD_{17}$ (baseline to post treatment), ROIs were registered to each participant's pre- and post-treatment scan, extracting a mean time series of the masked seed region. An initial fixed effects general linear model was conducted to compare pre- and post-treatment connectivity for each subject. The results of these analyses were then examined at the group level to find voxels where change in functional connectivity in the seed regions was associated with change in depression symptoms. This analysis was conducted using FLAME mixed effects model and demeaned $HAMD_{17}$ change for each subject as a regressor in the general linear model.

Connectivity values between our seed and target regions were extracted by transforming masks of individual clusters into individual space and extracting z-score values from the relevant connectivity map. In the case of baseline correlations, values were extracted from individual subjects' baseline connectivity. For connectivity change analysis, between subjects correlations were performed by extracting values from individual subjects' pre vs post contrast map. Anatomical specificity of the extracted regions was ensured by masking the target with the anatomical map for the region from the Harvard-Oxford atlas (50% probability).

To test whether improved outcomes were associated with relative shifts between our dorsal and ventral ROIs, we compared correlations between HAMD change and connectivity between a given target region and our two ROI seed regions (dmPFC and sgACC). These tests were performed using the Hotelling's test for dependent correlations (Hotelling, 1940).

Recent work has suggested that small movements may have a greater impact on resting-state analyses than previously considered (Power et al, 2012). Thus, in addition to visual inspection for large-scale movements, we assessed the impact of micro-movements on our data. Specifically, given that our analyses assessed correlations between functional connectivity and a clinical outcome measure ($HAMD_{17}$ change), we tested whether micro-movement would systematically alter our findings due to a confound between this dependent measure and movement. Mean

Table I Activation Peaks for Regions where Baseline Connectivity was Associated with Treatment Response

Seed	Region and broadman area	MNI coordinates			Peak z-score
		X	Y	Z	
Anterior midcingulate	*Positive correlation*				
	Medial frontal gyrus (R), (BA11, BA47, BA25, and BA32)	16	30	− 24	3.3
	Subcallosal gyrus (L) (BA 24 and BA25) and medial frontal gyrus (L) (BA11)	− 6	28	− 18	3.2
	Medial frontal gyrus (L) and middle frontal gyrus (L)	− 22	38	− 20	3
	Negative correlation				
	Putamen (R)	28	4	2	3.4
	Thalamus (R), medial dorsal N, and ventral lateral N	14	− 12	8	3.2
	Thalamus (L), medial dorsal N, VLN, VPN, and putamen	− 20	− 8	8	3.5
	Hippocampus (R) and amygdala	24	− 14	− 14	2.9
Subgenual cingulate	*Positive correlation*				
	Left paracingulate gyrus, medial frontal gyrus, (BA6, BA9, and BA32), and superior frontal gyrus (bi)	− 8	34	28	3.7
	Left middle frontal gyrus (BA8 and BA9)	− 32	14	38	3.6
	Right middle frontal gyrus and inferior frontal gyrus, (BA9)	44	18	28	3.2
	Negative correlation				
	Right insula, claustrum, and putamen	38	2	− 6	4
	Right parahippocampal gyrus and amygdala	20	− 6	− 16	3.9

Abbreviation: HAMD, Hamilton Depression Rating Scale.
Z-scores indicate the degree of correlation between connectivity and symptom improvement (HAMD reduction). Peaks are from significant clusters ($p < 0.05$ corrected).

relative movements were extracted from each subject at each time point. We then assessed correlations between movement and $HAMD_{17}$ change.

RESULTS

Clinical Results

Mean $HAMD_{17}$ score at baseline was 21.3 (± 6.7). Following dmPFC-rTMS treatment, mean $HAMD_{17}$ score had decreased significantly to 12.0 (± 8.2) ($p < 0.05$). Overall, $HAMD_{17}$ scores decreased by 45% (± 31%) between baseline and post treatment, although there was substantial interindividual variation in treatment response (Supplementary Figure S1).

Individuals with BPD ($n = 4$) had higher $HAMD_{17}$ scores at baseline (26.5 ± 4.1) than individuals with UPD ($n = 21$; 20.3 ± 1.30), although this difference did not reach significance ($t_{23} = 1.8$, $p = 0.08$). $HAMD_{17}$ change was greater in BPD (mean reduction of 12 ± 1.15) than UPD (mean reduction of 8.8 ± 1.51), but this difference was not significant ($t_{22} = 0.92$, $p = 0.37$).

Functional Connectivity Results

Baseline predictors of response. The stimulated dmPFC region contained a superior and an inferior subregion in the parcellation atlas of Craddock et al (Craddock et al, 2012); each one was investigated here. Baseline resting-state functional connectivity of the more superior dmPFC ROI seed was not significantly correlated with $HAMD_{17}$ change and will not be referred to further in this manuscript.

However, baseline functional connectivity of the more inferior dorsomedial (aMCC) ROI seed was significantly associated with treatment response (Table 1). Results reported for "dmPFC" will hereafter refer to this subregion specifically. Higher baseline connectivity between dmPFC and a medial prefrontal cluster spanning the subgenual cingulate gyrus (BA 25, 32) and ventromedial prefrontal cortex (BA 11, 47) was associated with better response to treatment. Lower baseline connectivity between dmPFC and right putamen, right thalamus (medial dorsal and ventral lateral subnuclei), and right hippocampus/amygdala was associated with better response to treatment. At baseline, connectivity of dmPFC with sgACC was primarily positive. Connectivity with thalamus and putamen was primarily negative (Table 1, Figure 1).

Baseline connectivity of sgACC was also significantly correlated with outcomes. Higher baseline connectivity between sgACC and dorsal lateral PFC (dlPFC—BA 8, 9) was associated with better response to treatment. Lower baseline connectivity between sgACC and the insula, putamen, and parahippocampus/amygdala was associated with better response to treatment. At baseline, connectivity of sgACC with dlPFC was primarily negative and connectivity with parahippocampus/amygdala was primarily positive. Subjects were split between positive and negative connectivity between sgACC and insula (Table 1, Figure 2).

Baseline connectivity between sgACC and parahippocampal gyrus was significantly correlated with baseline HAMD scores (− 0.42, $p < 0.05$). None of the other predictor regions was significantly correlated with baseline depression severity.

Neuroimaging results did not change in any substantial manner when individuals with bipolar disorder ($n = 4$) were
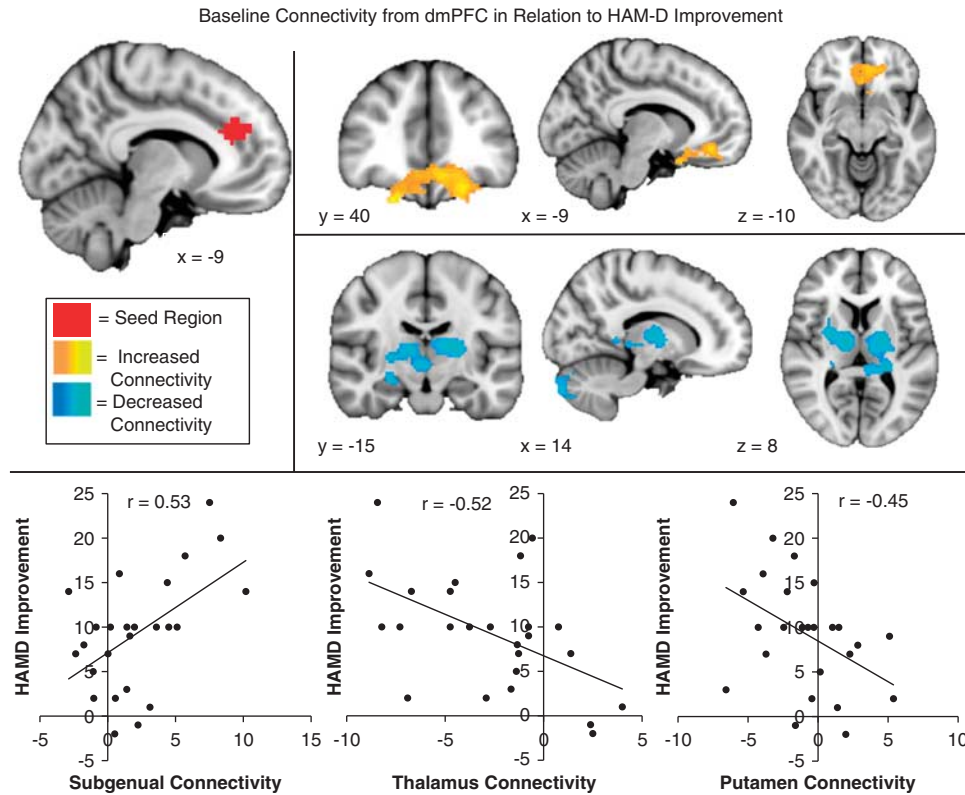
Baseline Connectivity from dmPFC in Relation to HAM-D Improvement

Figure 1 Baseline connectivity from dorsomedial prefrontal cortex (dmPFC) in relation to Hamilton Depression Rating Scale (HAMD) improvement: regions where high connectivity (orange) or low connectivity (blue) with the dmPFC seed (red) was significantly correlated with reduced depression (HAMD change, high scores indicate improvement) following repetitive transcranial magnetic stimulation (rTMS) to dmPFC.

excluded from either the baseline or change analysis (data not shown). This suggests that our results were not substantially driven by inclusion of individuals with bipolar disorder.

Neural correlates of response. There were a number of regions where connectivity change in response to rTMS was associated with outcomes (Supplementary Table S1). For the dmPFC seed, decreased connectivity with the bilateral insula and parahippocampal gyrus/amygdala was associated with better treatment response. The subjects who improved most appeared to have increased anti-correlations between dmPFC and insula. HAMD improvement was also associated with increased connectivity with the bilateral thalamus (medial dorsal nuclei and pulvinar)(Figure 3). On average, individuals who had the most improvement had high levels of anti-correlation at baseline, which were modified somewhat by treatment, whereas individuals had less successful outcomes had little connectivity in these regions (Table 2).

For the sgACC seed decreased connectivity with the ventral striatum and a region of dmPFC (just posterior to the initial seed region) were associated with better response to treatment (Figure 4). Subjects who responded well to treatment developed increased anti-correlation between sgACC and dmPFC. Subjects who responded less well to treatment showed increased positive correlation between sgACC and caudate (Table 2).

To examine whether outcomes were associated with relative dorsal-ventral shifts between our ROIs, we tested whether the association between HAMD change and connectivity change with target regions differed between the dorsal (dmPFC) and ventral (sgACC) ROIs. Connectivity change between dmPFC and thalamus was significantly correlated with $HAMD_{17}$ improvement. The corresponding correlation for the ventral ROI was nonsignificant ($r = 0.38$). These correlations were not significantly different from each other ($t = 0.7$, $p = 0.49$). Therefore, there is no basis for concluding that successful treatment is associated with a relative ventral-dorsal shift in cortico-thalamic connectivity. On the other hand, reduced connectivity between caudate and sgACC was associated with HAMD improvement. The corresponding correlation for the dorsal ROI was small ($r = -0.01$) and the difference with the sgACC correlation was marginally significant ($t = -2.01$, $p = 0.05$) suggesting that the successful treatment response corresponds with a relative shift in caudate connectivity with ventral (sgACC) as compared with dorsal (dmPFC) regions. The negative association between dmPFC-insula connectivity and outcome was significantly different from the corresponding sgACC connectivity ($r = 0.15$; $t = -2.36$, $p < 0.05$).

To test for confounding effects of micro-movements (Power *et al*, 2012), we examined whether relative displacement at either time point was associated with our dependent measure ($HAMD_{17}$ change). We found that relative movement was stable within individuals across time points ($r = 0.92$ for time 1 and time 2) but that $HAMD_{17}$ change was not correlated with movement at time 1 ($r = -0.11$) or time 2 ($r = -0.11$). Change in mean relative movement was also not related to $HAMD_{17}$ change ($r = -0.08$).

Baseline Connectivity from sgACC in Relation to HAM-D Improvement
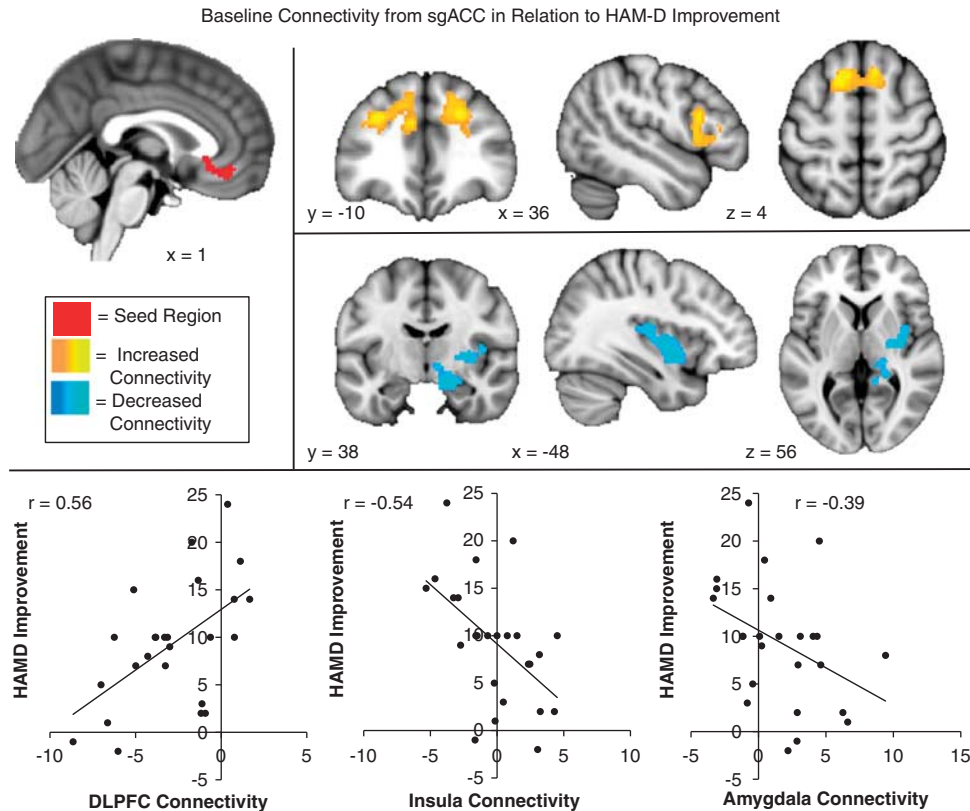

Figure 2 Baseline connectivity from subgenual cingulate cortex (sgACC) in relation to Hamilton Depression Rating Scale (HAMD) improvement: regions where high connectivity (orange) or low connectivity (blue) with the sgACC seed (red) was significantly correlated with reduced depression (HAMD change, high scores indicate improvement) following repetitive transcranial magnetic stimulation (rTMS) to dorsomedial prefrontal cortex (dmPFC).

DISCUSSION

This study examined neural predictors and correlates of treatment response to rTMS administered to the dmPFC in patients with MDD. Our primary aim was to find predictors of treatment response by identifying regions where baseline functional connectivity was associated with reduction in depression symptoms following treatment. Specifically, we examined whether baseline connectivity of the dmPFC target region with other brain regions was associated with successful outcomes. As resting-state activity of sgACC has been previously associated with treatment outcomes in depression (Davidson *et al*, 2003; Kennedy *et al*, 2001, 2007; Mayberg *et al*, 1997; Ritchey *et al*, 2011; Siegle *et al*, 2006), we also examined whether baseline connectivity of sgACC with other brain regions was correlated with treatment response. A secondary aim of this study was to examine neural correlates of treatment response, by identifying regions where change in functional connectivity with the dmPFC and sgACC from pre- to post-treatment correlated with reduction in depression symptoms.

As noted above, the degree of response to dmPFC-rTMS was strikingly heterogeneous, with individuals' HAMD$_{17}$ change varying widely. Our analysis of the neuroimaging data revealed a number of predictor regions, where connectivity with dmPFC and sgACC was associated with successful treatment response. Specifically, we found that patients with high baseline connectivity among cortical nodes involved in executive control and emotion

regulation (dmPFC-sgACC and sgACC-dlPFC) experienced a greater reduction in depressive symptoms following rTMS to the dmPFC. At the same time, patients with low baseline cortico-thalamic (dmPFC-medial dorsal thalamus), cortico-striatal (dmPFC-putamen), and cortico-limbic (sgACC-amygdala and sgACC-hippocampus) connectivity also experienced a greater response to the treatment (Figures 1 and 2).

We also observed a number of regions where connectivity changes correlated with improvement—that is, where the pre- to post-treatment change in functional connectivity to dmPFC and sgACC (Figures 3 and 4) was associated with reduction in depressive symptoms. Of particular interest, clinical improvement was associated with an increase in dmPFC-thalamus connectivity and a decrease in sgACC-caudate connectivity. Improvement was also associated with decreases in connectivity between dmPFC and insula, and between sgACC and a separate, more posterior region of midcingulate cortex. Concordance between the predictor and correlate regions observed here and circuits previously implicated in depression supports their plausibility as biomarkers for treatment response. Depression has been associated with functional and structural abnormalities in subgenual cingulate, thalamus, striatum, and limbic regions (Alcaro *et al*, 2010; Drevets *et al*, 2008; Heller *et al*, 2009, 2013; Mayberg, 2009; Phillips *et al*, 2003). Cortico-thalamic-striatal circuits have also shown signs of abnormal function in depression in recent studies. For example, sgACC connectivity with limbic, thalamic, and striatal regions has
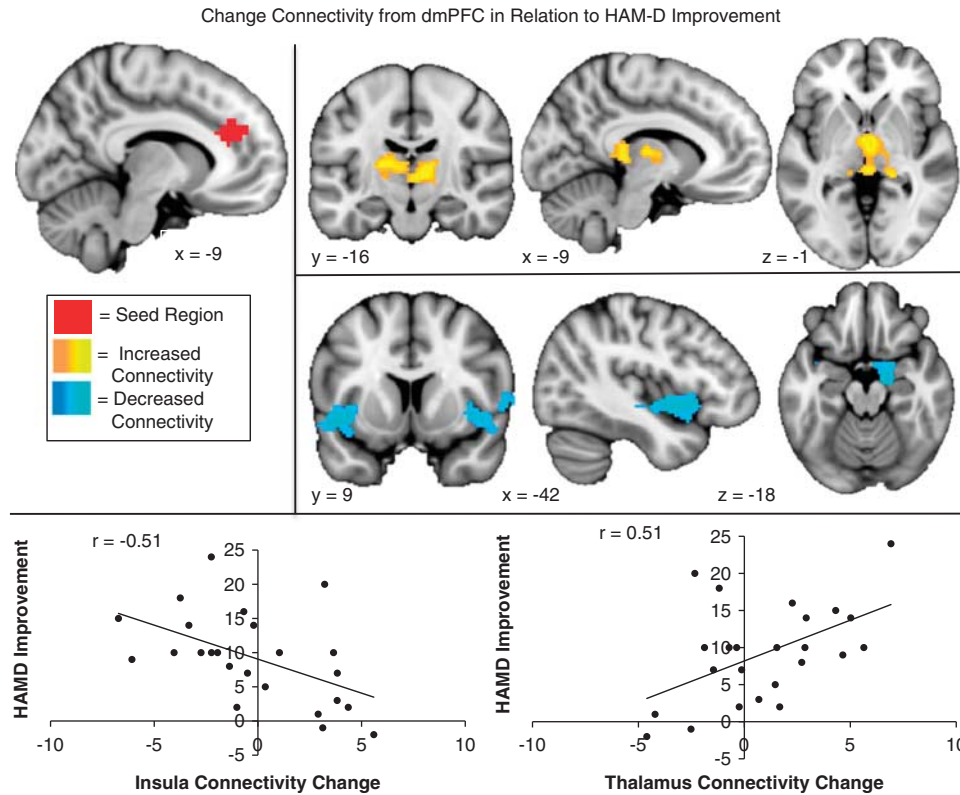
Change Connectivity from dmPFC in Relation to HAM-D Improvement

Figure 3 Change in connectivity from dorsomedial prefrontal cortex (dmPFC) in relation to Hamilton Depression Rating Scale (HAMD) improvement: regions where increased connectivity (orange) or decreased connectivity (blue) with the dmPFC seed (red) was significantly correlated with reduced depression (HAMD change, high scores indicate improvement) following repetitive transcranial magnetic stimulation (rTMS) to dmPFC.

been strongly implicated in the maladaptive emotion regulation underlying depression (Davey *et al*, 2012; Furman *et al*, 2011; Giacobbe *et al*, 2009; Lui *et al*, 2011) and associated with the degree of response to treatment (Anand *et al*, 2005, 2009; Diaconescu *et al*, 2011; Kozel *et al*, 2011).

Our predictor analysis suggests that specific patterns of connectivity may characterize those individuals who are most likely to benefit from rTMS to dmPFC. First, high levels of baseline cortico-cortical connectivity among prefrontal regions were found in the patients who had more successful outcomes. The association with high baseline connectivity between dmPFC and sgACC was of particular interest. Interplay between these regions has been associated with the transition between goal-directed cognition and affective response (Simpson *et al*, 2001a, b), and connectivity between similar regions has been implicated both with depressive symptomology (Davey *et al*, 2012) and response to antidepressant medication (Kozel *et al*, 2011). Given the role of this particular region of dmPFC in facilitating goal-directed behavior by integrating cognitive information with associated rewards and punishments (Shackman *et al*, 2011), the association between positive outcomes and high baseline connectivity between this region and the sgACC and low baseline connectivity with striatum may suggest that positive outcomes are associated with the capacity for executive control over core emotional functions. In the context of this interpretation, it is noteworthy that improvements in treatment were associated with increased connectivity between dmPFC and thalamus,

and decreased connectivity between sgACC and the caudate. What is suggested is that a potential mechanism of action of rTMS to dmPFC is increased influence of cognitive control networks over thalamic and striatal regions, possibly linked with improved facilitation of goal-directed behavior (Corbetta and Shulman, 2002; Price and Drevets, 2010; Sheline *et al*, 2010).

What remains unclear is whether the outcome-predicting patterns of functional connectivity in the present study represent general biomarkers of response across all treatment modalities or more specific biomarkers for response to dorsomedial rTMS in particular. The network-based model of major depression proposed by Seminowicz *et al* (Seminowicz *et al*, 2004) suggests that different antidepressant approaches might work through different neural routes, suggesting that the predictors and correlates of change here may be specific for response to rTMS treatment, or even more specifically rTMS to this specific site (dmPFC). In line with such an interpretation, it is noteworthy that Kozel *et al* (Kozel *et al*, 2011) found that baseline connectivity of similar cingulate regions was associated with response to antidepressant medication, but that the association was in the opposite direction to that observed here. One intriguing possibility is that connectivity of these regions might differentiate between suitability for a particular modality of treatment (see Supplementary Discussion for expanded discussion).

The ability to predict successful treatment response based on reliable biomarkers would allow for optimal matching between patient and treatment and may therefore represent

Table 2 Connectivity and HAMD17 Values for Each Subject

(A)
DMPFC Seed

HAMD change	Time 1 insula	Time 2 insula	Time 1 thalamus	Time 2 thalamus	Time 1 MCC	Time 2 MCC	Time 1 caudate	Time 2 caudate
24	0.53	− 2.43	− 8.44	− 0.93	5.5	3.36	3.58	1.52
20	− 1.27	3.31	− 0.57	− 2.36	− 4.49	6.25	− 1.54	4.46
18	− 0.78	− 4.38	− 1.17	− 4.77	3.42	2.34	− 1.76	2.27
16	3.06	2.42	− 8.86	− 6.69	5.34	8.82	− 3.49	− 3.55
15	3.01	− 4.68	− 4.49	0.3	9.49	4.94	1.17	− 0.5
14	0.29	− 3.81	− 4.74	− 3.64	5.15	3.31	1.65	2.18
14	− 0.64	− 1.87	− 6.72	− 0.58	4.88	5.26	6.57	3.69
10	− 3.06	2.46	− 7.3	1.08	3.32	3.48	4.97	6.8
10	4.71	3.38	− 4.74	− 7.76	3.33	11.37	6.98	1.31
10	3.75	0.16	− 3.76	− 3.83	3.81	2.12	0.67	− 1.16
10	4.04	2.26	− 8.22	− 0.82	10.55	2.32	− 5.72	0.53
10	1.42	2.63	0.75	− 0.71	5.36	10.02	6.26	1.19
10	− 2.32	− 7.93	− 2.71	− 3.64	6.56	0.62	2.76	− 1.11
9	4.25	− 1.06	− 0.77	4.26	4.41	0.89	5.89	3.38
8	1.99	0.82	− 1.34	1.68	2.7	5.33	− 0.3	0.43
7	2.55	1.67	− 1.27	− 4.08	2.56	11.71	1.14	10.03
7	− 5.89	− 2.66	1.38	1.66	− 1.35	6.93	2	7.59
5	− 1.6	− 1.16	− 1.39	0.16	4.52	3.33	5.46	0.34
3	− 6.47	− 0.52	− 1.65	− 1.92	1.38	4.51	− 0.57	6.65
2	3.67	0.62	− 2.92	− 1.27	8.18	5.47	8.26	2.93
2	− 2.89	2.15	− 6.91	− 2.95	10.23	8.83	5.75	− 0.91
1	2.77	5.44	4	− 1.57	6.06	6.52	4.89	0.33
− 1	− 3.27	− 0.77	2.38	1.13	3.7	5.21	− 0.02	1.72
− 2	− 1.47	4.52	2.5	− 1.4	4.39	8.23	2.67	5.57
Correlation with HAMD change	0.21	− 0.35	− 0.53	− 0.22	− 0.16	− 0.22	− 0.26	− 0.17
Average ⩾10	0.98	− 0.65	− 4.69	− 2.64	4.79	4.94	1.7	1.36
Average <10	− 0.58	0.82	− 0.54	− 0.39	4.25	6.09	3.2	3.46

(B)
sgACC seed

HAMD change	Time 1 MCC	Time 2 MCC	Time 1 caudate	Time 2 caudate	Time 1 insula	Time 2 insula	Time 1 thalamus	Time 2 thalamus
24	− 0.92	− 3.6	− 3.36	2.94	− 1.39	− 3.37	− 9.69	− 0.07
20	− 3.30	− 0.04	2.81	− 0.86	1.36	3.12	− 2.46	− 0.12
18	1.69	1.19	− 0.84	0.56	0.19	0.36	0.57	− 1.13
16	− 1.57	− 3.13	− 1.31	4.84	− 2.4	− 0.58	0.94	0.84
15	2.42	− 3.3	− 3.86	3.17	− 3.29	0.98	− 1.19	− 0.57
14	− 2.41	− 2.73	− 0.18	− 1.1	− 1.1	− 1.32	1.86	2.05
14	4.06	− 5.05	− 6.1	7.81	1.85	− 2.88	− 4.72	− 3.06
10	− 1.45	− 0.59	2.36	− 1.94	3.92	− 2.64	− 4.96	− 0.71
10	− 0.65	− 10.04	− 6.86	8.86	3.62	− 3.12	− 2.59	7.94
10	0.1	− 7.16	− 4.32	− 0.6	− 0.86	− 7.61	0.68	− 0.34
10	1.93	3.08	0.28	2.84	5.09	3.21	− 0.47	3.55
10	0.91	2	0.31	2	0.4	2.04	− 4.87	− 2.65
10	3.76	− 0.59	− 2.59	1.41	2.99	5.67	− 2.07	3.62
9	− 1.25	2.25	2.45	0.83	− 3.37	0.09	0.52	0.55
8	3.02	− 1.73	− 3.28	5.99	3.42	4.21	3.49	− 2.34
7	2.52	4.73	1.81	2.62	2.36	6.82	− 2.81	− 0.93
7	5.27	2.92	− 1.63	9.05	2.88	− 1.68	2.05	− 1.43

Table 2 (Continued)

(A)
DMPFC Seed

HAMD change	Time 1 insula	Time 2 insula	Time 1 thalamus	Time 2 thalamus	Time 1 MCC	Time 2 MCC	Time 1 caudate	Time 2 caudate
5	− 0.8	2.54	2.56	− 7.21	− 2.38	− 0.17	− 3.08	− 0.02
3	1.85	4.94	3.05	2.11	0.49	7.46	− 2.18	2.85
2	4.35	− 0.48	− 1.29	3.46	3.91	4.27	− 1.01	0.66
2	− 1.26	− 3.7	− 0.39	2.19	4	0.88	3.02	0.36
1	0.72	2.25	2.12	− 0.25	3.31	1.03	0.44	− 1.69
− 1	− 3.02	3.67	7.25	4.35	− 0.86	5.33	2.31	− 0.69
− 2	− 0.31	8.78	8.68	0.35	3.28	4.91	− 0.88	− 2.85
Correlation with HAMD change	− 0.12	− 0.48	− 0.52	0.05	− 0.37	− 0.44	− 0.43	0.08
Average ⩾10	0.35	− 2.3	− 1.82	2.3	0.8	− 0.47	− 2.23	0.72
Average <10	1.01	2.38	1.94	2.14	1.55	3.01	0.17	− 0.5

Abbreviations: DMPFC, dorsomedial prefrontal cortex; HAMD, Hamilton Depression Rating Scale; MCC, midcingulate; sgACC, subgenual cingulate cortex.
Connectivity values for the dmPFC (A) and sgACC (B) seeds (extracted *z*-scores for each target region). Subjects are ranked by $HAMD_{17}$ change scores. At bottom are correlations between connectivity and $HAMD_{17}$ change scores for each time point. In addition, the mean connectivity value for subjects above (⩾10) and below (<10) the median $HAMD_{17}$ change score is provided.
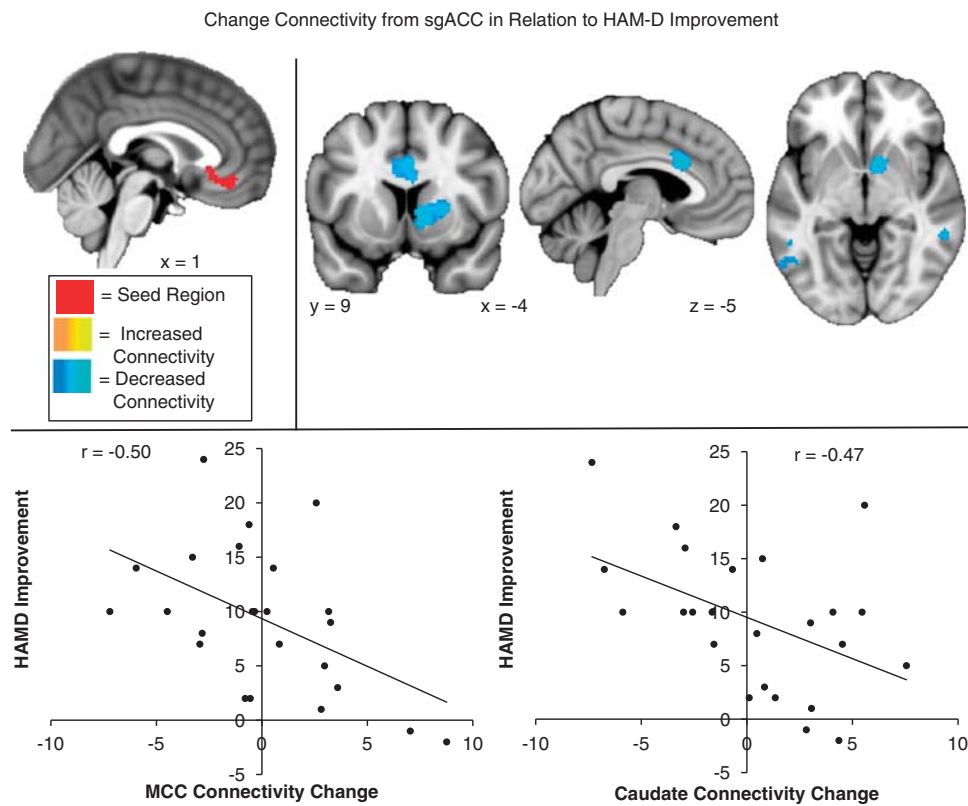
Figure 4 Change in connectivity from subgenual cingulate cortex (sgACC) in relation to Hamilton Depression Rating Scale (HAMD) improvement: regions where decreased connectivity (blue) with the sgACC seed (red) was significantly correlated with reduced depression (HAMD change, high scores indicate improvement) following repetitive transcranial magnetic stimulation (rTMS) to dorsomedial prefrontal cortex (dmPFC).

a key breakthrough in improving treatment outcomes. Here we demonstrate that baseline connectivity of dmPFC and sgACC with each other and with other cortical, thalamic, and striatal regions was associated with successful response to treatment with dmPFC-rTMS. A further step toward the goal of establishing the clinical utility of these findings would be to test the model outlined here in an independent sample of depressed individuals. We would predict that individuals with low levels of baseline connectivity between dmPFC, thalamus, and striatum and high levels of connectivity between dmPFC and sgACC would be most likely to benefit from rTMS to dmPFC. If these predictions

prove correct, comparison with rTMS treatments applied to other therapeutic targets (eg, dlPFC) would further demonstrate specificity of these biomarkers (Downar and Daskalakis, 2012). This approach, if successful, would represent a promising step toward the goal of developing reliable biological markers for predicting the treatment with the greatest likelihood of success in any given patient.

REFERENCES

Alcaro A, Panksepp J, Witczak J, Hayes DJ, Northoff G (2010). Is subcortical-cortical midline activity in depression mediated by glutamate and GABA? A cross-species translational approach. *Neurosci Biobehav Rev* 34: 592–605.

Anand A, Li Y, Wang Y, Lowe MJ, Dzemidzic M (2009). Resting state corticolimbic connectivity abnormalities in unmedicated bipolar disorder and unipolar depression. *Psychiatry Res* 171: 189–198.

Anand A, Li Y, Wang Y, Wu J, Gao S, Bukhari L *et al* (2005). Antidepressant effect on connectivity of the mood-regulating circuit: an FMRI study. *Neuropsychopharmacology* 30: 1334–1344.

Beckmann CF, Jenkinson M, Smith SM (2003). General multilevel linear modeling for group analysis in FMRI. *Neuroimage* 20: 1052–1063.

Chen R, Gerloff C, Classen J, Wassermann EM, Hallett M, Cohen LG (1997). Safety of different inter-train intervals for repetitive transcranial magnetic stimulation and recommendations for safe ranges of stimulation parameters. *Electroencephalogr Clin Neurophysiol* 105: 415–421.

Collins PY, Patel V, Joestl SS, March D, Insel TR, Daar AS *et al* (2011). Grand challenges in global mental health. *Nature* 475: 27–30.

Corbetta M, Shulman GL (2002). Control of goal-directed and stimulus-driven attention in the brain. *Nat Rev Neurosci* 3: 201–215.

Craddock RC, James GA, Holtzheimer PE 3rd, Hu XP, Mayberg HS (2012). A whole brain fMRI atlas generated via spatially constrained spectral clustering. *Hum Brain Mapp* 33: 1914–1928.

Davey CG, Harrison BJ, Yücel M, Allen NB (2012). Regionally specific alterations in functional connectivity of the anterior cingulate cortex in major depressive disorder. *Psychol Med* 42: 2071–2081.

Davidson RJ, Irwin W, Anderle MJ, Kalin NH (2003). The neural substrates of affective processing in depressed patients treated with venlafaxine. *Am J Psychiatry* 160: 64–75.

Diaconescu AO, Kramer E, Hermann C, Ma Y, Dhawan V, Chaly T *et al* (2011). Distinct functional networks associated with improvement of affective symptoms and cognitive function during citalopram treatment in geriatric depression. *Hum Brain Mapp* 32: 1677–1691.

Downar J, Daskalakis ZJ (2012). New targets for rTMS in depression: A review of convergent evidence. *Brain Stimul* 6(3): 231–240.

Downar J, Sankar A, Giacobbe P, Woodside B, Colton P (2012). Unanticipated rapid remission of refractory bulimia nervosa, during high-dose repetitive transcranial magnetic stimulation of the dorsomedial prefrontal cortex: a case report. *Front Psychiatry* 3: 30.

Drevets WC, Savitz J, Trimble M (2008). The subgenual anterior cingulate cortex in mood disorders. *CNS Spectr* 13: 663–681.

Fox MD, Snyder AZ, Vincent JL, Corbetta M, Essen DC, Van, Raichle ME (2005). The human brain is intrinsically organized into dynamic, anticorrelated functional networks. *Proc Natl Acad Sci USA* 102: 9673–9678.

Furman DJ, Hamilton JP, Gotlib IH (2011). Frontostriatal functional connectivity in major depressive disorder. *Biol Mood Anxiety Disord* 1: 11.

Gartlehner G, Hansen RA, Morgan LC, Thaler K, Lux L, Van Noord M *et al* (2011). Comparative benefits and harms of second-generation antidepressants for treating major depressive disorder: an updated meta-analysis. *Ann Intern Med* 155: 772–785.

Giacobbe P, Mayberg HS, Lozano AM (2009). Treatment resistant depression as a failure of brain homeostatic mechanisms: implications for deep brain stimulation. *Exp Neurol* 219: 44–52.

Harmer CJ, Thilo KV, Rothwell JC, Goodwin GM (2001). Transcranial magnetic stimulation of medial-frontal cortex impairs the processing of angry facial expressions. *Nat Neurosci* 4: 17–18.

Heller AS, Johnstone T, Light SN, Peterson MJ, Kolden GG, Kalin NH *et al* (2013). Relationships between changes in sustained fronto-striatal connectivity and positive affect in major depression resulting from antidepressant treatment. *Am J Psychiatry* 170: 197–206.

Heller AS, Johnstone T, Shackman AJ, Light SN, Peterson MJ, Kolden GG *et al* (2009). Reduced capacity to sustain positive emotion in major depression reflects diminished maintenance of fronto-striatal brain activation. *Proc Natl Acad Sci USA* 106: 22445–22450.

Hotelling H (1940). The selection of variates for use in prediction with some comments on the general problem of nuisance parameters. *Annals of Mathematical Statistics* 11: 271–283.

Imel ZE, Malterer MB, McKay KM, Wampold BE (2008). A meta-analysis of psychotherapy and medication in unipolar depression and dysthymia. *J Affect Disord* 110: 197–206.

Jenkinson M, Bannister P, Brady M, Smith S (2002). Improved optimization for the robust and accurate linear registration and motion correction of brain images. *Neuroimage* 17: 825–841.

Kapur S, Phillips AG, Insel TR (2012). Why has it taken so long for biological psychiatry to develop clinical tests and what to do about it? *Mol Psychiatry* 17: 1174–1179.

Kennedy SH, Evans KR, Krüger S, Mayberg HS, Meyer JH, McCann S *et al* (2001). Changes in regional brain glucose metabolism

measured with positron emission tomography after paroxetine treatment of major depression. *Am J Psychiatry* **158**: 899–905.

Kennedy SH, Konarski JZ, Segal ZV, Lau MA, Bieling PJ, McIntyre RS *et al* (2007). Differences in brain glucose metabolism between responders to CBT and venlafaxine in a 16-week randomized controlled trial. *Am J Psychiatry* **164**: 778–788.

Kozel FA, Rao U, Lu H, Nakonezny PA, Grannemann B, McGregor T *et al* (2011). Functional connectivity of brain structures correlates with treatment outcome in major depressive disorder. *Front Psychiatry* **2**: 7.

Li C-T, Wang S-J, Hirvonen J, Hsieh J-C, Bai Y-M, Hong C-J *et al* (2010). Antidepressant mechanism of add-on repetitive transcranial magnetic stimulation in medication-resistant depression using cerebral glucose metabolism. *J Affect Disord* **127**: 219–229.

Lui S, Wu Q, Qiu L, Yang X, Kuang W, Chan RCK *et al* (2011). Resting-state functional connectivity in treatment-resistant depression. *Am J Psychiatry* **168**: 642–648.

Mayberg HS (2009). Targeted electrode-based modulation of neural circuits for depression. *J Clin Invest* **119**: 717–725.

Mayberg HS, Brannan SK, Mahurin RK, Jerabek PA, Brickman JS, Tekell JL *et al* (1997). Cingulate function in depression: a potential predictor of treatment response. *Neuroreport* **8**: 1057–1061.

Murray CJ, Lopez AD (1996). Evidence-based health policy–lessons from the Global Burden of Disease Study. *Science* **274**: 740–743.

Northoff G, Wiebking C, Feinberg T, Panksepp J (2011). The "resting-state hypothesis" of major depressive disorder-a translational subcortical-cortical framework for a system disorder. *Neurosci Biobehav Rev* **35**: 1929–1945.

Papakostas GI, Thase ME, Fava M, Nelson JC, Shelton RC (2007). Are antidepressant drugs that combine serotonergic and noradrenergic mechanisms of action more effective than the selective serotonin reuptake inhibitors in treating major depressive disorder? A meta-analysis of studies of newer agents. *Biol Psychiatry* **62**: 1217–1227.

Phillips ML, Drevets WC, Rauch SL, Lane R (2003). Neurobiology of emotion perception II: Implications for major psychiatric disorders. *Biol Psychiatry* **54**: 515–528.

Pizzagalli D, Pascual-Marqui RD, Nitschke JB, Oakes TR, Larson CL, Abercrombie HC *et al* (2001). Anterior cingulate activity as a predictor of degree of treatment response in major depression: evidence from brain electrical tomography analysis. *Am J Psychiatry* **158**: 405–415.

Power JD, Barnes KA, Snyder AZ, Schlaggar BL, Petersen SE (2012). Spurious but systematic correlations in functional connectivity MRI networks arise from subject motion. *Neuroimage* **59**: 2142–2154.

Price JL, Drevets WC (2010). Neurocircuitry of mood disorders. *Neuropsychopharmacology* **35**: 192–216.

Ritchey M, Dolcos F, Eddington KM, Strauman TJ, Cabeza R (2011). Neural correlates of emotional processing in depression: changes with cognitive behavioral therapy and predictors of treatment response. *J Psychiatr Res* **45**: 577–587.

Seminowicz DA, Mayberg HS, McIntosh AR, Goldapple K, Kennedy S, Segal Z *et al* (2004). Limbic-frontal circuitry in major depression: a path modeling metanalysis. *Neuroimage* **22**: 409–418.

Shackman AJ, Salomons TV, Slagter HA, Fox AS, Winter JJ, Davidson RJ (2011). The integration of negative affect, pain and cognitive control in the cingulate cortex. *Nat Rev Neurosci* **12**: 154–167.

Sheline YI, Price JL, Yan Z, Mintun MA (2010). Resting-state functional MRI in depression unmasks increased connectivity between networks via the dorsal nexus. *Proc Natl Acad Sci USA* **107**: 11020–11025.

Siegle GJ, Carter CS, Thase ME (2006). Use of FMRI to predict recovery from unipolar depression with cognitive behavior therapy. *Am J Psychiatry* **163**: 735–738.

Simpson JR Jr, Drevets WC, Snyder AZ, Gusnard DA, Raichle ME (2001a). Emotion-induced changes in human medial prefrontal cortex: II. During anticipatory anxiety. *Proc Natl Acad Sci USA* **98**: 688–693.

Simpson JR Jr, Snyder AZ, Gusnard DA, Raichle ME (2001b). Emotion-induced changes in human medial prefrontal cortex: I. During cognitive task performance. *Proc Natl Acad Sci USA* **98**: 683–687.

Smith SM (2002). Fast robust automated brain extraction. *Hum Brain Mapp* **17**: 143–155.

Spielmans GI, Berman MI, Usitalo AN (2011). Psychotherapy versus second-generation antidepressants in the treatment of depression: a meta-analysis. *J Nerv Ment Dis* **199**: 142–149.

Terao Y, Ugawa Y, Enomoto H, Furubayashi T, Shiio Y, Machii K *et al* (2001). Hemispheric lateralization in the cortical motor preparation for human vocalization. *J Neurosci* **21**: 1600–1609.

Zhang Y, Brady M, Smith S (2001). Segmentation of brain MR images through a hidden Markov random field model and the expectation-maximization algorithm. *IEEE Trans Med Imaging* **20**: 45–57.

Supplementary Information accompanies the paper on the Neuropsychopharmacology website (http://www.nature.com/npp)